The 9th European Congress on Computational Methods in Applied Sciences and Engineering
ECCOMAS Congress 2024
3–7 June 2024, Lisboa, Portugal

INTEGRATION OF TOPOLOGY OPTIMIZATION AND SIZING OPTIMIZATION TECHNIQUES FOR ADVANCED ORTHOTIC DESIGN

DHAVAL PATEL[1,3], THOMAS ROCKENBAUER[2], THOMAS ANTRETTER[3], SANDRA SCHLOEGL[1] AND MARGIT LANG[1]

[1] Polymer Competence Center Leoben GmbH, 8700 Leoben, Austria
e-mail: Dhaval.rasheshkumar.patel@pccl.at

[2] Luxinergy GmbH, 8700 Leoben, Austria

[3] Montanuniversität Leoben, Chair of Mechanics, 8700 Leoben, Austria

Key words: Wrist Splint, Finite Element Analysis (FEA), Additive Manufacturing (AM), Topology Optimization (TO), Sizing Optimization (SO)

Summary. Wrist splints, a key element in post-trauma or post-surgery care, are indispensable for providing crucial rigid support, facilitating healing, alleviating pain, and ensuring precise anatomical alignment. Despite their critical role the conventional manufacturing process, utilizing low-temperature thermoplastic materials shaped to fit the injured area, is plagued by inherent limitations. This research pioneers a transformative approach to address these shortcomings by integrating modern technologies such as Finite Element Analysis (FEA), and Additive Manufacturing (AM). Augmented by a customization paradigm involving 3D scanning and virtual design optimization through computer-aided engineering, the methodology ensures a tailored fit to the patient's unique anatomy. Significantly, the integration of topology optimization and sizing optimization techniques becomes pivotal in achieving an optimal distribution of stiff and soft materials respectively in hand orthosis design. This two-step optimization approach begins with the Topology Optimization (TO) of the outer stiff material shell and concludes with the Sizing Optimization (SO) of the inner soft material layer, finely tuned for hand orthosis. This innovative orthotic design paradigm not only enhances material efficiency, reduces weight, and enables patient-specific customization but also propels advancements in orthotic design research. In conclusion, integrating state-of-the-art technologies such as FEA and modern AM methods are expected to significantly improve recovery outcomes.

1 INTRODUCTION

Wrist splints serve as integral orthopedic interventions, offering mechanical support and stability across a spectrum of musculoskeletal conditions such as sprains, strains, fractures, and tendonitis. Their significance extends to the post-surgical phase, where they contribute to the bio-mechanical facilitation of healing processes and protective stabilization of the wrist. Notably, wrist splints are commonly prescribed in the management of carpal tunnel syndrome and the attenuation of repetitive strain injuries, functioning to sustain a neutral wrist position and thereby diminish undue pressure on nerves and tendons [1, 2]. Moreover, their therapeutic utility encompasses arthritis management by providing biomechanical reinforcement and mitigating inflammatory responses, highlighting the multifaceted role of wrist splints in clinical orthopedics. The three most common types of wrist splints, volar, thumb spica,

and sugar tong, serve distinct purposes based on their design and structure [3]. Volar splints, positioned on the palm side of the wrist, are often used for sprains, strains, or mild fractures, providing support while allowing some movement. Thumb spica splints, incorporating support for the thumb along with the wrist, are frequently employed in cases of thumb injuries, such as sprains or fractures. Sugar tong splints, extending from below the elbow to the hand, are utilized for more severe wrist injuries or fractures, offering enhanced stability by immobilizing both the wrist and forearm [4]. The choice of splint type depends on the nature and severity of the wrist condition, demonstrating the tailored approach in orthopedic care.

Crafting custom-fitting splints by hand using low-temperature thermoplastics is a detailed and skillful process [5]. It involves carefully shaping the material to perfectly match the unique contours of a person's body [6]. While this hands-on method is great for making personalized splints, it has some challenges. It takes a lot of time and skill, making it hard to produce many splints quickly. Also, the materials used may not be as durable, and creating intricate designs can be tricky, affecting how well the splint works. Aspects like aesthetics, wear comfort (i.e., avoidance of pressure sores, breathability of the orthosis) as well as problems associated with proper cleaning of the orthosis in daily usage are known reasons why patients may feel uncomfortable in wearing orthosis during prescribed time. A significant challenge within existing splint designs arises from the inadequate incorporation of biomechanical considerations during the structural design phase and predominant reliance on empirical-based design principles, particularly in areas such as integration of skin breathing holes, and adjustments to material increments or reductions. These challenges lead to the risk of potential splint damage. Finding the right balance between providing support and ensuring comfort for the patient is another tough aspect of this manual approach [7].

To overcome the above mentioned limitations of traditional manual manufacturing methods, research is increasingly focusing on personalized patient care using refined and technology-assisted approaches such as CAE Optimization and 3D printing. These technological advances promise greater precision, reproducibility, and manufacturing efficiency in the field of orthopedic customization [8].

Structural optimization [9] is a method used in engineering and design to determine the most effective material layout and shape of a structure, considering specific design criteria and constraints. This technique originated in the 1980s and has progressed as technology has advanced. The primary techniques for structural optimization includes TO [10, 11], which optimizes material distribution for desired structural performance; shape optimization [12], which enhances design geometry to improve performance and SO [13], which determines optimal component dimensions. By utilizing TO, engineers can design structures that are stronger, lighter, and more efficient, while meeting performance requirements such as durability and stability. This results in reduced material waste and improved structural performance, leading to cost savings and environmental benefits. The use of TO is expanding in various fields, including aerospace [14], automotive [15], civil and biomedical engineering [16]. In the area of product design and manufacturing, sizing optimization is also crucial for developing products that are not only aesthetically pleasing but also functionally effective [17]. Achieving the right balance of size and proportions can impact usability, user experience, and overall product performance.

Despite the potential benefits, research involving FEA and TO in AM splint design remains limited, primarily focusing on spinal and lower limb applications, such as the Boston brace, fracture stabiliza-

tion splints, or plaster casts. There is a notable scarcity of research regarding TO applied to functional wrist splint design combined with AM. Given the functional nature of wrist splints, a biomechanically based design is imperative. Therefore, there is a need for a clinically applicable orthosis design and manufacturing framework incorporating AM and TO to bridge this gap [18, 19].

2 MATERIALS AND OPTIMIZATION PROCEDURE

2.1 Materials and properties

The 3D-printed hand orthosis comprises two distinct materials: a rigid (outer shell) and a flexible (inner shell), developed by materials experts at Luxinergy GmbH. The rigid outer shell, classified as Luxinergy's ductile resin, possesses high biocompatibility and is suitable for 3D printing using Digital Light Processing (DLP) technology. This material exhibits appropriate elasticity and bending strength to withstand mechanical loads while providing structural support (Table 1). In turn, the flexible inner shell is made of a Luxinergy's elastomer resin material, that is characterized by its flexibility and softness. This highly recommended material is also biocompatible and suitable for 3D printing, ensuring wear comfort and facilitating easy donning and doffing without direct contact between the rigid outer shell and the hand.

Table 1: Material properties.

	Stiff (rigid) material	Soft (flexible) material
Young's modulus	2200 MPa	1 MPa
Poisson's ratio	0.35	0.35

2.2 Scanning and modeling

3D wrist scanning was conducted utilizing the Einstar 3D Scanner (Shining 3D, China) on a healthy 27-year-old male subject (height: 166 cm, weight: 65 kg), with the subject maintaining a steady resting position on the table while employing the assistance of their second hand to stabilize the limb, aiming to minimize movement-induced distortions. Throughout the scanning procedure, the subject endeavored to maintain a pain-free position, with the scanner circumnavigating the limb 360° to capture its geometrical features. The acquisition of the entire limb's data typically required 2-3 minutes. Subsequent to scanning, post-processing was performed utilizing software (Exstar V1.05.0, Shining 3D, China), wherein the relevant region was delineated for orthotic adaptation, and extraneous anatomical components, such as the metacarpophalangeal joint, were excised from the scan data, yielding a polyhedral model. Subsequent remeshing procedures were executed to achieve uniform surface partitioning utilizing Rhino 7 software (McNeel Inc., USA). The creation of offsets from the base hand model and the generation of orthotic models with increased thickness were also carried out using Rhino 7 software. The orthotic length was set at approximately 235 mm, constituting approximately one-third of the subject's limb length, aiming to strike a balance between functionality and structural integrity. The design incorporated an open upper part to facilitate requisite flexibility, ventilation, and ease of use, while concurrently ensuring optimal support and stability during functional movements. To mitigate direct skin contact with rigid orthotic materials and enhance comfort during donning and doffing, the model was offset by 1 mm outwards (as shown in Figure 1, Design 1), with a soft material layer (1.5 mm) utilized as padding beneath the rigid structure (as shown in Figure 1, Design 3). Initial thickness specifications for the orthotic stiff

material were established at 2.0 mm to optimize weight reduction while maintaining requisite mechanical robustness. The resultant solid orthotic model was subsequently subjected to FEA for optimization purposes.

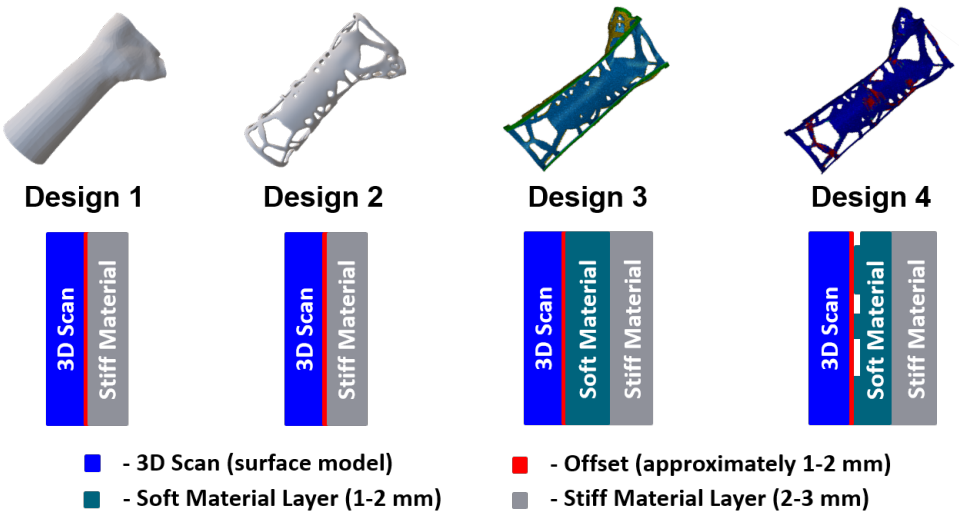

Figure 1: Visualization of stiff and soft materials placement with consideration of offset from 3D scan in different design variants.

2.3 Loads and boundary conditions

In FEA studies of hand orthoses, a variety of loads are employed to assess their structural integrity and biomechanical response, simulating real-world usage scenarios. These loads mainly include static, dynamic, bending, impact, and thermal loads, each representing distinct forces and stresses encountered during daily activities and environmental conditions. Static loads replicate the weight of the hand and external objects, while dynamic loads mimic movement forces during gripping and manipulation. Bending loads simulate flexion and extension motions of the hand and wrist, and impact loads replicate sudden and high-intensity forces, such as those from falls or collisions. Additionally, thermal loads simulate temperature fluctuations affecting material properties. Through comprehensive load analysis, the orthosis's capacity to deliver support, stability, and comfort can be assessed, guiding design improvements to enhance functionality and user satisfaction. Within the current study an extensive literature research was conducted to identify suitable loads and boundary conditions tailored to the specific requirements of orthotic devices. After a thorough examination of various options, two distinct types of loads and boundary conditions were adapted from previous studies.

2.3.1 Static load and constraints

The corrective force exerted on the upper limb aims to reduce strain, enhance joint stability, and promote proper joint alignment during arthritis treatment. The primary source of this force stems from extensive contact pressure between the hand brace and the hand. To precisely measure this contact pressure, Force Sensing Resistor (FSR) sensors were utilized to capture the force exerted during the resting position. This is extensively described in the research conducted by Wei Yan et al. [19]. Given

that the corrective force is influenced by both strap tension and tight contact at specific regions, the pressure distribution was measured at 22 key positions of anatomy, as depicted in Figure 2 and Table 2. However, to streamline the data acquisition process, certain low-pressure regions were excluded from consideration. As for boundary conditions, full constraints were applied to the edge near the strap to simulate tightening, while the lower edge of the hand orthosis was fixed in all six degrees of freedom.

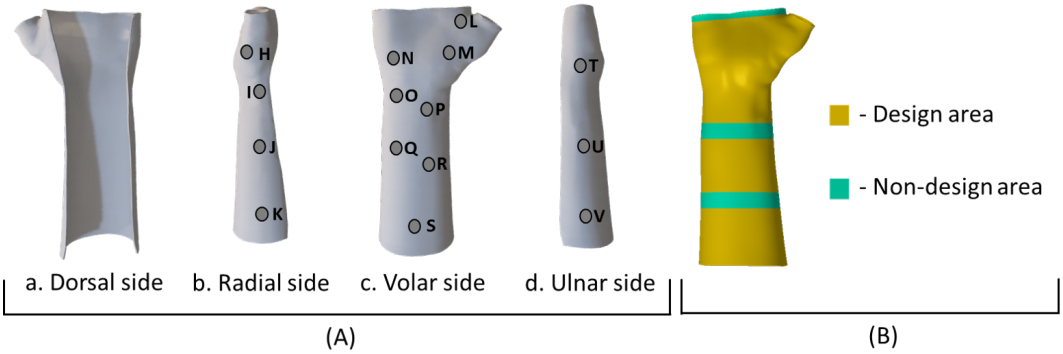

Figure 2: A) Regions where contact pressure was measured according to [19] and B) Design and non-design area of hand orthosis geometry.

Table 2: Contact force measured at specific regions [19].

Position	Force (N)	Position	Force (N)
H	68.32 ± 0.56	P	63.44 ± 0.27
I	86.01 ± 0.51	Q	34.16 ± 0.02
J	73.81 ± 0.07	R	53.07 ± 0.02
K	95.16 ± 0.13	S	39.04 ± 0.18
L	31.72 ± 0.08	T	48.19 ± 0.21
M	73.81 ± 0.09	U	32.94 ± 0.04
N	92.11 ± 0.29	V	26.84 ± 0.02
O	03.66 ± 0.01		

2.3.2 Bending load and constraints

The design and materials of hand orthosis significantly influence how bending loads are managed, dictating the orthosis's ability to resist deformation and provide support to the hand and wrist. Bending loads primarily arise from hand and wrist movements, especially during activities involving flexion, extension, or rotation of the wrist joint. The wrist strength during various movements is evaluated using static (isometric) and dynamic (isokinetic) tests conducted on volunteers. Previous studies, including those by Jessie Marie et al. [20] and Scott Delp et al. [21], have reported the maximum torques for flexion-extension and radial-ulnar deviation that healthy volunteers can generate. Caution is required with regard to the interpretation of strength data determined on healthy persons and their conversion to strength data for arthritis-damaged wrists. Amis et al. [22] found that the elbow flexion strength of rheumatoid arthritis patients was approximately 45% of that observed in healthy individuals during wrist movements. However, Aitor Cazon et al. [23] argue that in real-life scenarios, arthritis patients may not consistently exert maximum strength, potentially risking splint breakage. To address this concern,

analyses in this study were conducted at 8% of the maximum isometric strength of a healthy individual. Subsequently, finite element simulations were also performed using 50% of the maximum strength of a healthy individual, incorporating a factor of safety to mitigate risks. To mitigate stress concentrations arising from point forces and to simulate a more realistic interaction between the orthosis and the hand/wrist, the force values obtained (refer to Table 3) were strategically applied to the splint surfaces intended to bear such forces in practical scenarios (as illustrated in Figure 3). For further insights into these loading conditions and constraints, readers are referred to the prior study [23]. In this simulation, the forearm was considered to be at rest, while the upper end of the wrist, including the fingers, was allowed to move freely. As for constraints, the rear surfaces of the orthosis were immobilized in all six degrees of freedom for the four movements under investigation (highlighted in blue color in Figure 3). Additionally, to replicate the interaction between the forearm and the orthosis, and to represent three-point bending boundary conditions, the middle surfaces of the orthosis were constrained during each specific wrist movement (highlighted in orange color in Figure 3).

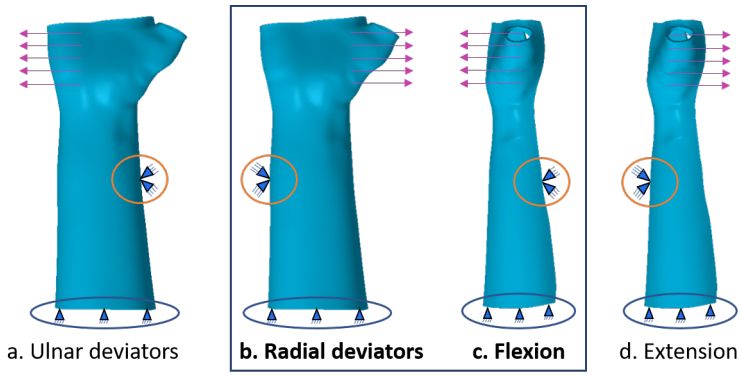

Figure 3: Load and constraints in the hand orthosis for the four main wrist movements.

Table 3: Considered torque and loads applied to the hand orthosis for the four main movements [23].

	Torque (N m)	Applied 8% loads (N)	Applied 50% loads (N)
Flexors	14.8	11.9	73.7
Extensors	8.4	6.7	41.4
Radial deviators	11.4	9.1	56.4
Ulnar deviators	9.9	7.9	48.9

2.4 Optimization workflow

The optimization workflow begins with 3D scanning and the creation of a 3D model from the surface model, as depicted in Figure 4. These steps are detailed in the previous section, ”Scanning and Modeling.” Following this, static linear FEA was conducted on the base model (Design 1, Figure 1) using ABAQUS 2019 to assess the performance of the orthosis. The base model, fabricated from the biocompatible Luxinergy’s ductile resin material, served as the foundation for this analysis. The results obtained from the static linear FEA served as a validation benchmark for subsequent optimization endeavors. The optimization of the hand orthosis was delineated into two distinct parts, each serving a specific purpose.

Initially, stiff material topology optimization (TO) was employed to enhance mechanical support. This strategy aimed to refine the distribution of stiff materials within the orthotic design, thereby improving its structural integrity and load-bearing capacity. To achieve this, the objective function of the optimization was to maximize the stiffness of the model while satisfying the volume constraint. This optimization strategy aligning with the bending load and constraints introduced in the previous section, given their significance in necessitating mechanical support from the orthosis. In the TO process, the orthosis edges were designated as non-design areas to uphold the structural integrity of the orthosis. This decision ensured that critical regions remained intact, facilitating the effective transmission of mechanical support throughout the orthotic structure. Notably, the TO was executed across three distinct volume fractions: 50%, 55%, and 60%. This variation in volume fractions allowed for the exploration of different material distributions, enabling the identification of optimal configurations that strike a balance between mechanical support and material efficiency.

Secondly, soft material sizing optimization was undertaken to enhance comfort during usage. By optimizing the sizing and distribution of soft materials within the orthotic structure, this approach sought to mitigate discomfort and pressure points commonly associated with orthotic wear. The same objective function used in TO was applied here, as maximizing stiffness indirectly fulfills the objective of reducing pressure sores in the design. By segmenting the optimization process into these two parts, the study aimed to address both mechanical performance and user comfort, thereby ensuring a comprehensive and balanced orthotic design.

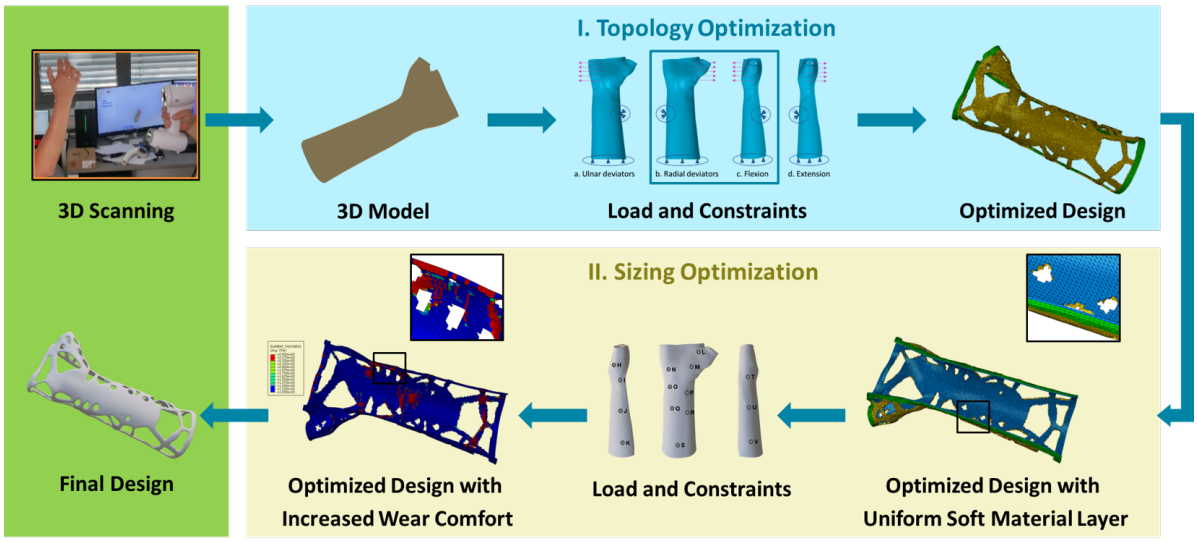

Figure 4: Integrated optimization workflow.

3 RESULTS

The optimization results for hand orthosis models are displayed in Figure 5. Three load steps, flexion, radial deviation, and contact pressure, were implemented in FE setup (Figure 5A). For wrist movements like flexion and radial deviation, 50% of the load was applied (Table 3). TO was conducted with retained volume of 50%, 55%, and 60% of the base model (Design 1, Figure 1), resulting in distinct designs (Fig-

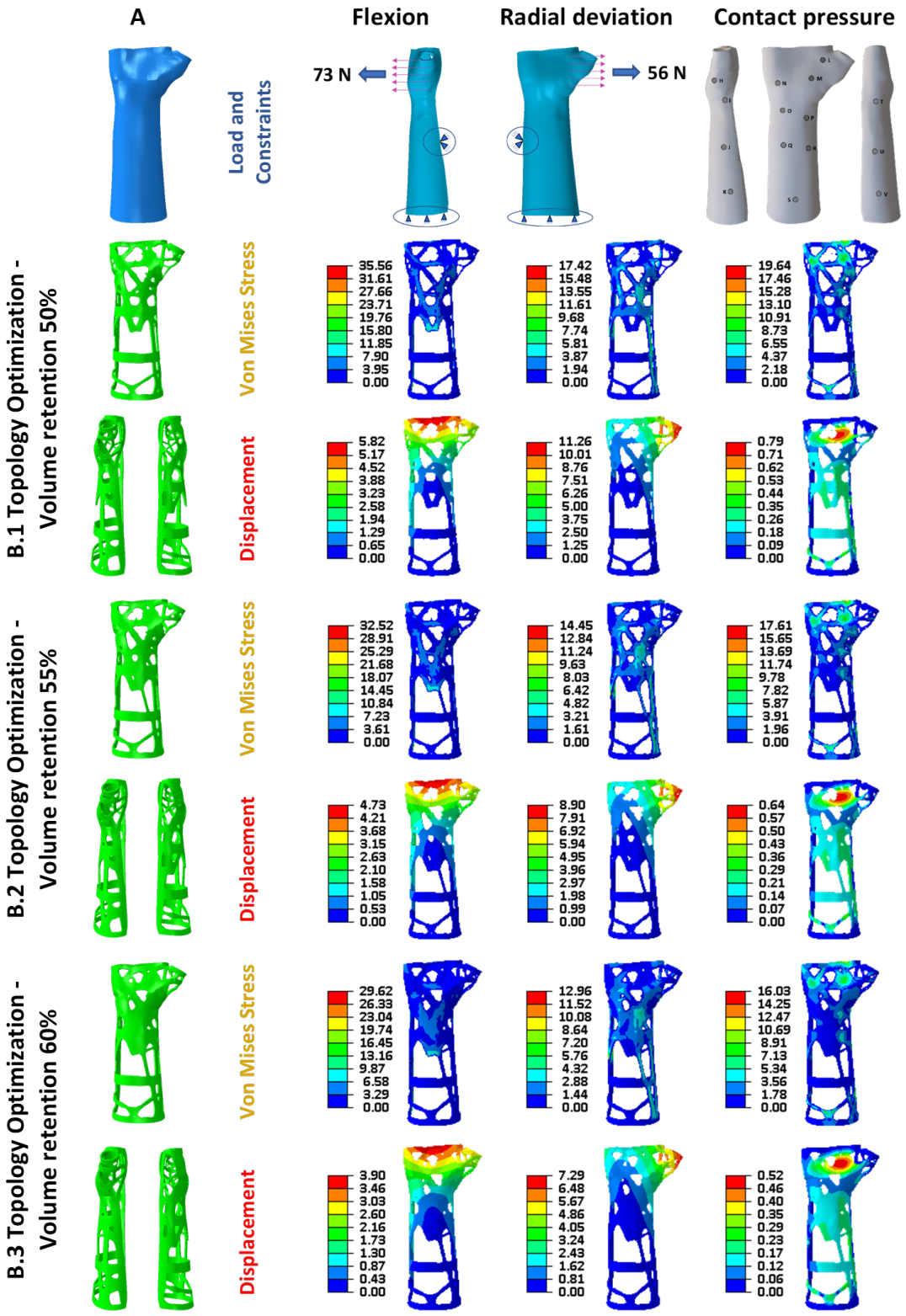

Figure 5: A) Loads and constraints for three different load steps, B) Topology optimization for different volume retentions.

ure 5 B.1-B.3). Below 50% volume retention, the designs exhibited discontinuous truss-like structures, leads to the critical transition point in optimization.

In Figure 6, a bar chart depicts the maximum displacement for all three load steps across various volume retentions. Notably, a comparative analysis with the reference paper [23] indicates a higher level of stiffness in our results under equivalent loading conditions. Furthermore, under contact pressure loading, the optimized models with 60% volume retention exhibit maximum displacements of 0.52 mm. This value is below the maximum allowable displacement for clinical orthoses, set at 2.5 mm by [19], highlighting the efficacy of the optimized design (with 60% volume retention) in meeting clinical standards and ensuring adequate support and stability with a safety factor of 5.

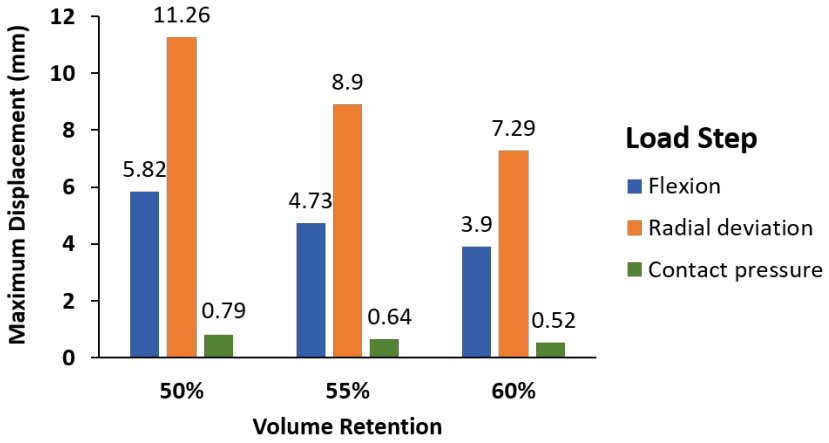

Figure 6: Maximum displacement of orthosis under various load step across different volume retention.

Following the analysis of three distinct variants of topology-optimized hand orthosis, the orthosis featuring 60% volume retention was selected for further investigation due to its lightweight construction, enhanced breathability, and overall structural integrity. In Figure 7, finite element results of the full hand model are compared with this optimized hand orthosis under an 8% load, as outlined in Table 3.

Subsequent to TO, the focus shifted towards sizing optimization to enhance wear comfort. The objective of the sizing optimization process is to alleviate contact pressure at specific regions, as illustrated in Figure 2, by strategically augmenting the soft layer between the hand and the stiff geometry in those areas. This targeted adjustment aims to optimize the distribution of pressure across the interface, thereby enhancing overall comfort and functionality. Initially, a uniform 1.5 mm thick soft material layer was added beneath the optimized stiff material geometry. Through sizing optimization, the soft material layer thickness was varied from a minimum of 1.3 mm or 1.0 mm to a maximum of 2 mm in two distinct simulation scenarios, as depicted in Figure 8A and Figure 8B respectively. Figure 8 illustrates the contour plot of element thickness for the soft material layer in both simulation cases. Notably, in Simulation 2 (Figure 8B), where the minimum thickness constraint was set to 1 mm, a greater coverage of regions with a thick soft layer is observed compared to Simulation 1 (Figure 8A), where the minimum thickness constraint was set to 1.3 mm. These findings highlight the impact of minimum thickness constraints on the distribution and coverage of the soft material layer, underscoring the importance of parameter selection in optimizing orthotic design for enhanced wear comfort and functionality.

Following the finalization of the sizing optimization, two distinct geometries representing the stiff material and soft material components were converted into .stl (Standard Triangle Language) files, aligning with the initial requirements for 3D printer manufacturing of Multi-Material hand orthoses. This crucial step marks the transition from virtual design to tangible production, laying the foundation for the fabrication of orthoses tailored to individual patient needs.

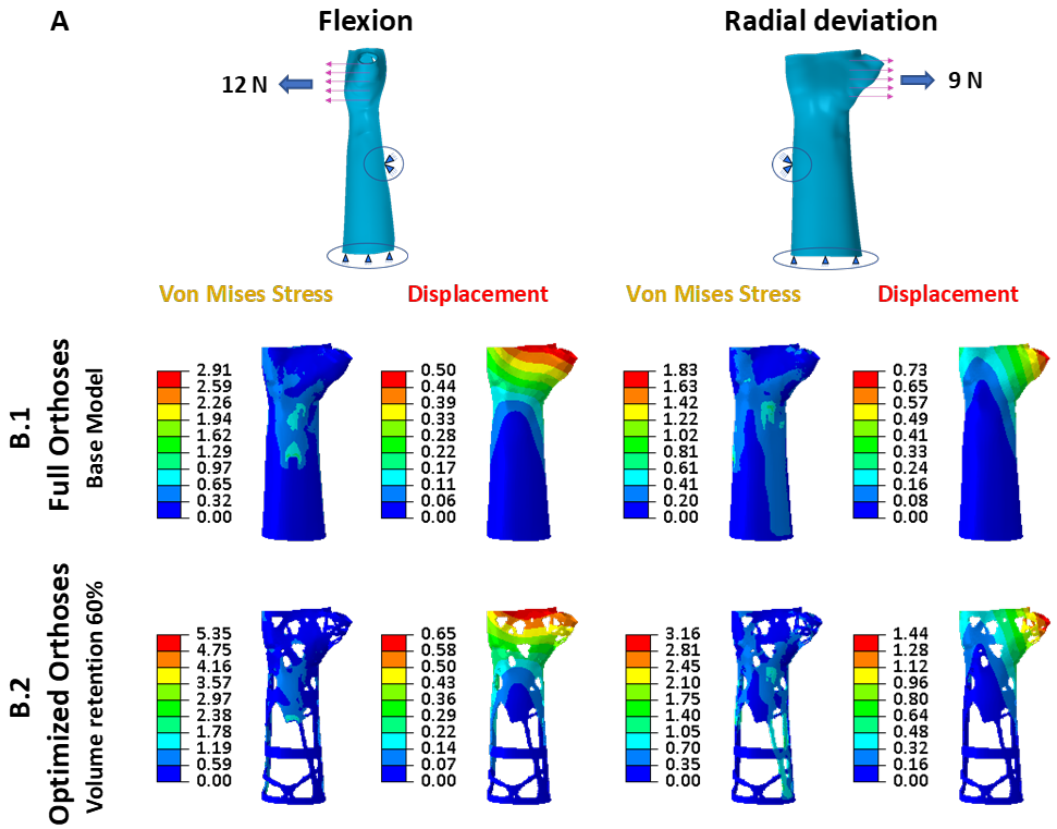

Figure 7: A) Load and constraint for flexion and radial deviation, B) Optimization result of full orthosis (base model) and optimized orthosis (volume retention 60%)

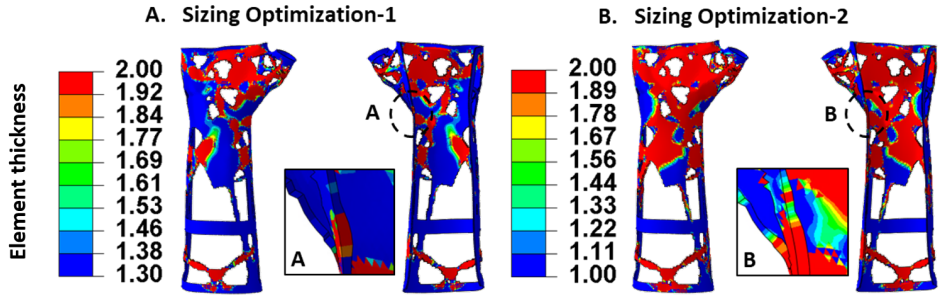

Figure 8: Sizing optimization with different constraint on minimum element thickness 1.3 mm (A) and 1 mm (B).

4 CONCLUSION

This paper presents an integrated optimization strategy for custom-designed wrist splints, with a dual focus on providing minimal mechanical support and optimizing wear comfort. In conclusion, the optimization of hand orthosis models demonstrated significant advancements in structural integrity and comfort. The TO across various volume retentions revealed that the 60% retention model fulfilled specific requirements by outperforming previous designs and meeting clinical standards for displacement limits. SO further enhanced wear comfort by strategically varying the thickness of the soft material layer to alleviate contact pressure, with the most effective distribution achieved in the scenario with a 1 mm minimum thickness constraint. These optimized designs were successfully translated into manufacturable .stl files for multi-materials, highlighting their practical applicability in producing lightweight, breathable, and supportive orthosis tailored to individual patient needs. There remains further potential to enhance design efficiency in terms of material utilization and user convenience by refining the parameters employed in both TO and SO methodologies.

ACKNOWLEDGEMENTS

The part of the research was conducted within the production of the future project "3DFit4Wear" (project number: 891254), which received funding from the Austrian Research Promotion Agency (FFG). The research work was also performed within the COMET-project 'Photostructurable Encapsulation Molds and Magnetic Composites' (project-no.: VII-S2) at the Polymer Competence Center Leoben GmbH (PCCL, Austria) within the framework of the COMET-program of the Federal Ministry for Climate Action, Environment, Energy, Mobility, Innovation and Technology and the Federal Ministry for Digital and Economic Affairs with contributions by the Graz University of Technology. The PCCL is funded by the Austrian Governments and the State Governments of Styria, Lower Austria and Upper Austria.

References

[1] Lucia Ramsey, Robert John Winder, and Joseph G McVeigh. The effectiveness of working wrist splints in adults with rheumatoid arthritis: a mixed methods systematic review. *Journal of rehabilitation medicine*, 46(6):481–492, 2014.

[2] Teresa Sadura-Sieklucka, Beata Sokolowska, Agnieszka Prusinowska, Anna Trzaska, and Krystyna Ksiezopolska-Orlowska. Benefits of wrist splinting in patients with rheumatoid arthritis. *Reumatologia/Rheumatology*, 56(6):362–367, 2018.

[3] Steven F DeFroda, Joseph A Gil, Steven Bokshan, and Gregory Waryasz. Upper extremity quad splint: indications and technique. *The American Journal of Emergency Medicine*, 33(12):1818–1822, 2015.

[4] Devin M Howell, Samuel Bechmann, and Philipp J Underwood. Wrist splint. *National Library of Medicine*, 2020.

[5] David Palousek, Jiri Rosicky, Daniel Koutny, Pavel Stoklásek, and Tomas Navrat. Pilot study of the wrist orthosis design process. *Rapid prototyping journal*, 20(1):27–32, 2014.

[6] Ulrich Mennen. A simple, comfortable, conforming, and adaptable splint. *The Journal of hand surgery*, 14(3):576–578, 1989.

[7] Sam Chi Chung Chan, Tom Chun Wai Tsoi, Chiu Tai Yip, Lisa Ho, and et al. Comparison of effects of prefabricated soft wrist orthosis and conventional wrist thermoplastic splint on symptoms

of carpel tunnel syndrome. *JPO: Journal of Prosthetics and Orthotics*, 35(4):283–290, 2023.

[8] Mo Zhou, Changning Sun, Seyed Ataollah Naghavi, Ling Wang, Maryam Tamaddon, Jinwu Wang, and Chaozong Liu. The design and manufacturing of a patient-specific wrist splint for rehabilitation of rheumatoid arthritis. *Materials & Design*, 238:112704, 2024.

[9] Peter W Christensen and Anders Klarbring. *An introduction to structural optimization*, volume 153. Springer Science & Business Media, 2008.

[10] Martin Philip Bendsoe and Ole Sigmund. *Topology optimization: theory, methods, and applications*. Springer Science & Business Media, 2013.

[11] Dhaval Patel, Thomas Rockenbauer, Sandra Schlögl, and Margit Lang. Single and multi-material topology optimization of continuum structures: Abaqus plugin. *Mathematical Modeling in Physical Sciences: 12th IC-MSQUARE, Belgrade, Serbia*, pages 3–17, August 28–31, 2023.

[12] M Hasan Imam. Three-dimensional shape optimization. *International Journal for Numerical Methods in Engineering*, 18(5):661–673, 1982.

[13] Mesut Baran and Felix F Wu. Optimal sizing of capacitors placed on a radial distribution system. *IEEE Transactions on power Delivery*, 4(1):735–743, 1989.

[14] Ji-Hong Zhu, Wei-Hong Zhang, and Liang Xia. Topology optimization in aircraft and aerospace structures design. *Archives of computational methods in engineering*, 23:595–622, 2016.

[15] RJ Yang, Ching-Hung Chuang, Xiangdong Che, and Ciro Soto. New applications of topology optimisation in automotive industry. *International Journal of Vehicle Design*, 23(1-2):1–15, 2000.

[16] Taimoor Iqbal, Ling Wang, Dichen Li, Enchun Dong, Hongbin Fan, Jun Fu, and Cai Hu. A general multi-objective topology optimization methodology developed for customized design of pelvic prostheses. *Medical engineering & physics*, 69:8–16, 2019.

[17] D Wang, WH Zhang, and JS Jiang. Truss optimization on shape and sizing with frequency constraints. *AIAA journal*, 42(3):622–630, 2004.

[18] Tz-How Huang, Chi-Kung Feng, Yih-Wen Gung, Mei-Wun Tsai, Chen-Sheng Chen, and Chien-Lin Liu. Optimization design of thumbspica splint using finite element method. *Medical and Biological Engineering and Computing*, 44:1105–1111, 2006.

[19] Wei Yan, Mao Ding, Bo Kong, XiaoBing Xi, and Mingdong Zhou. Lightweight splint design for individualized treatment of distal radius fracture. *Journal of medical systems*, 43:1–10, 2019.

[20] Jessie Marie Vanswearingen. Measuring wrist muscle strength. *Journal of Orthopaedic & Sports Physical Therapy*, 4(4):217–228, 1983.

[21] Scott L Delp, Anita E Grierson, and Thomas S Buchanan. Maximumisometric moments generated by the wrist muscles in flexion-extension and radial-ulnar deviation. *Journal of biomechanics*, 29(10):1371–1375, 1996.

[22] AA Amis, S Hughes, JH Miller, V Wright, and D Dowson. Elbow joint forces in patients with rheumatoid arthritis. *Rheumatology*, 18(4):230–234, 1979.

[23] Aitor Cazon, Sarah Kelly, and et al. Analysis and comparison of wrist splint designs using the finite element method: Multi-material three-dimensional printing compared to typical existing practice with thermoplastics. *Proceedings of the Institution of Mechanical Engineers, Part H: Journal of Engineering in Medicine*, 231(9):881–897, 2017.